General and Comparative Endocrinology 338 (2023) 114275

Contents lists available at ScienceDirect

General and Comparative Endocrinology

journal homepage: www.elsevier.com/locate/ygcen

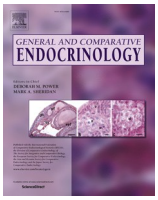

Comparative transcriptomic analysis and genome-wide characterization of the Semaphorin family reveal the potential mechanism of angiogenesis around embryo in ovoviviparous black rockfish (*Sebastes schlegelii*)

Bingyan Zheng [1], Likang Lyu [1], Xiaojie Wang, Haishen Wen, Yun Li, Jianshuang Li, Yijia Yao, Chenpeng Zuo, Shaojing Yan, Songyang Xie, Xin Qi [*]

Key Laboratory of Mariculture, Ministry of Education, Ocean University of China, Qingdao, China

ARTICLE INFO

Keywords:
Transcriptomic
Ovoviviparity
Angiogenesis
Semaphorin

ABSTRACT

To guarantee the quality and survival rate of their offspring, ovoviviparous teleost evolved special characteristics of in vivo fertilization and embryo development. Maternal black rockfish, having over 50 thousand embryos developing within the ovary simultaneously, provided around 40% nutrition throughout oocyte development, while the capillaries around each embryo contributed the rest 60% during pregnancy. Since fertilization, capillaries started to proliferate and developed into a placenta-like structure that covered over half of each embryo. Aimed to characterize the potential mechanism behind, comparative transcriptome analysis of samples collected according to the process of pregnancy. Three important time point in the process, including mature oocyte stage, fertilization and sarcomere period, were chosen for the transcriptome sequencing. Our study identified key pathways and genes involved in the cell cycle as well as DNA replication and repair, cell migration and adhesion, immune, and metabolic functions. Notably, several of the semaphoring gene family members were differently expressed. To confirm the accuracy of these genes, total of 32 *sema* genes were identified from the whole genome and distinct expression pattern of *sema* genes was observed in different pregnant stages. Our results revealed a novel insight for further investigating the functions of *sema* genes in reproduction physiology and embryo processes in ovoviviparous teleost.

1. Introduction

Reproduction, one of the most crucial biological activities during the life cycle, is the only way to guarantee the continuation of the species. With the largest population of vertebrates, fishes have evolved a variety of reproduction strategies including oviparity, viviparity and ovoviviparity to acclimate their living environment (Juntti and Fernald, 2016). Oviparity, the most common breeding strategy in teleost, allows the eggs fertilized outside themother. While, different from oviparous fish, fertilization and early development took place in the ovary or the uterus-like organ of maternal body of viviparity and ovoviviparity species (Lodé, 2012). After early development, the free-swimming larva were breed by the female fish through parturition process (Rheubert et asl., 2014). The phenotype varied with the evolution from oviparous to viviparous fish in both the morphological structure and the physiological process, including the disappearance of zygote egg shell, prolongation of embryonic development time, maternal nutrition to the embryo, inhibition of the maternal immune rejection of embryos (Graham et al., 2011; Heulin et al., 2005; Murphy and Thompson, 2011; Packard et al., 1977; Thompson et al., 2000; Thompson and Speake, 2006), etc. Such breeding strategy protected the embryo from fluctuations in environmental factors such as temperature, oxygen content, osmotic pressure and pH, as well as from predation (Gross, 2005; Shine, 1989).

Another significant characteristic of viviparous animal was the nutrition resource throughout the embryo development. The embryo not only depend upon the yolk provide, however, additionally from the mother through the blood vessel system. In mammals, the placenta, located at the interface of the vascular bed between the maternal and the fetus, had developed and played irreplaceable role in embryonic development including the effectively transportation of nutrition, oxygen information communication, discharge of metabolic waste and

* Corresponding author at: College of fishery, Ocean University of China, Qingdao, China.
E-mail address: qx@ouc.edu.cn (X. Qi).
[1] Bingyan Zheng and Likang Lyu contributed equally to this work.

https://doi.org/10.1016/j.ygcen.2023.114275
Received 10 January 2023; Received in revised form 16 March 2023; Accepted 17 March 2023
Available online 20 March 2023

carbon dioxide (Schindler and Hamlett, 1993). In the course of evolution, similar organs with variations were discovered in animals from different kingdoms performing similar functions. In reptiles and avian, placenta-like organs are evolutionarily conducive to maintaining moist and warm embryos during the evolution from sea to land and sky (Power and Schulkin, 2012). During embryo development in marsupials, a monolayer structure was developed by trophoblast cells around the embryo, which may represent the formation of the original placenta (Renfree, 2010). While in mammals, generated by the chorionic membrane, the placenta and umbilical cord ensured adequate nutrition sources and an appropriate environment for the growth of the offspring (Maltepe and Fisher, 2015). It is clear that placenta is an evolutionary adaptation beneficial to the vertebrates in terms of evolutionary relationship, and its structure and species have been studied to be diverse (Roberts et al., 2016). However, in ovoviviparous animals, less is known about the interaction and the pathway of exchange of nutrition, oxygen and information between the mother and the embryo (Gilmore et al., 1983.). The increase in the fetal requirement for nutrients and oxygen in early development is usually accompanied by a continuous augment in angiogenesis and blood flow volume (Gude et al., 2004). Angiogenesis, the generation of new vessels germinated from existing vessels, is strictly and precisely regulated by diversified cells included endothelial cells (ECs), vascular smooth muscle cells (VSMCs) and perivascular cells (PCs) (Carmeliet, 2005; Folkman, 1995; He et al., 2021; Krüger-Genge and Franke, 2019; Yin et al., 2012) and requires the functional activities of coordinated varied hormones and guidance molecules in microenvironment. Notably, during the fetal development, angiogenesis is regulated by hormonal variations such as increased levels of estrogen (Hanahan and Folkman, 1996; Turner et al., 2003). For example, endothelial cells expressing estrogen receptors can be affected by the estrogen stimulation during pregnancy (Losordo and Isner, 2001). Endothelial tip cells (ETCs) are the navigators of the sprouts. Steer the follow-up of the ECs by sensing the attractive or repulsive cues such as VEGFs or semaphorins (Melincovici et al., 2018; Sakurai et al., 2012). Semaphorins, as a large family of extracellular signaling molecules, play essential roles in the development of blood vessels by mediating cell-to-cell communication (Alto and Terman, 2017a). It has been well demonstrated that estrogen levels up-regulate Sema3F transcription in utero, particularly in the connective tissue that envelops intrauterine blood vessels (Richeri et al., 2011). Loss-of-function of semaphorins result in developmental defects and even death (Hota and Buck, 2012; Tran et al., 2007), it is of interest to investigate whether semaphorins is important to the formation of capillaries around embryo.

Black rockfish (*Sebastes schlegelii*) is an ovoviviparous teleost with both fertilization and embryo development happened inside the ovary (Wang et al., 2021). During gestation, approximately 70% of the catabolic energy is contributed by the maternal system (Boehlert and Yoklavich, 1984), indicating a direct communication between the maternal and the embryo. Anatomical observations of pregnant black rockfish show that the surface of each fertilized egg is covered with abundant capillaries which may play the role for the nutrition and oxygen transfer and information communication.

Ovoviviparous black rockfish was employed as the research model in this study to understand the potential mechanisms under laying the formation of capillaries following fertilization. For the transcriptome sequencing, ovary samples from three distinct developmental stages (without oocytes or embryos) were chosen. The identification of semaphorins, structures of sequences, phylogenetic relationships, evolutionary characteristics, and expression pattern at the genome-wide level were then systematically analyzed. These findings will offer new insights into the molecular mechanism of semaphorins in placental angiogenesis as well as fresh perspectives on teleost reproduction and evolution of the reproductive strategy.

2. Materials and methods

2.1. Ethics statement

All animal experiments were reviewed and approved by the Animal Protection and Utilization Institutional Committee of Ocean University of China. The protocol of animal care and handling used in this study was approved by the Animal Experimental Ethics Committee of Ocean University of China prior to the study. The studies did not involve endangered or protected species. All experiments were carried out in accordance with relevant guidelines and regulations. In simple terms, individuals were anesthetized with 3-aminobenzoate methanesulfonic acid (MS-222, 0.2 g/L, Beijing Green Hengxing Biotechnology, Beijing, China) and then quickly decapitated with spinal scissors to reduce the animal's suffering.

2.2. Sample preparation and pregnant stage identification

In total, 27 female black rockfish at different pregnant stages were collected from the North Yellow Sea, Shandong province, China in April 2021. Under laboratory conditions, individuals were kept separately in water tank (diameter 1 m, height 1.5 m) for 2 days without feeding. After anesthetization with MS-222, ovary of each individual from late April to late May was separated and the developmental period of oocyte/embryo was observed to identify the precise pregnant stages by a microtome (Leica, Wetzler, Germany). The oocyte in mature stage (**M**) was fully mature but unfertilized. After fertilized in vivo, fertilized eggs developed germinal disc and classified as fertilized stage (**F**). along the development, myomere were observed in embryo during sarcomere stage (**S**, **Supplementary Fig. S1**).

2.3. RNA extraction, Library construction and transcriptome sequencing

Total RNA of the ovarian tissues was extracted using TRIzol Reagent kit (Invitrogen, CA, USA) after ground by a tissue lyser (DHS Life Science & Technology, Beijing, China). Total RNA integrity was determined by the RNA Nano 6000 Assay Kit of the 2100 Bioanalyzer System (Agilent Technologies, CA, USA).

To minimize the difference between replicates, equal amounts of total RNA from 3 individuals at the same pregnant stage were grouped together. Nine sequenced libraries were generated using the NEBNext®Ultra™ RNA Library Prep Kit for Illumina® (NEB, Ipswich, Massachusetts, USA) and an index code was added to the attribute sequence for each sample. The index-coded samples were sequenced on an Illumina HiSeq X Ten platform, acquiring 150 bp of paired-end reads. The raw sequence has been submitted to the National Center for Biotechnology Information's (NCBI) Short Read Archive database (PRJNA820964).

2.4. Sequence data processing and differentially expressed genes analysis

Raw data obtained from RNA-seq were first qualified by FastQC software (https://www.bioinformatics.babraham.ac.uk/projects/fastqc/). To acquire clean, high quality readings, original raw reads with quality scores below 20 (q-value $\leq$ 20) were filtered by Fastp (version 0.22.0) (Chen et al., 2018). Subsequently, the filtered reads from each sample were mapped to the reference *Sebastes schlegelii* genome in NCBI (PRJNA516036) by Hisat2 (version 2.1.0) on paired-end model (Kim et al., 2019). The quantification analysis of assembled reads from each sample was accomplished using StringTie (version 2.2.0) (Pertea et al., 2015) in a reference-based approach and quantify transcript abundances. The transcript level of all genes was normalized according to the fragments per kilobase per million mapped reads (FPKM). Different expression analysis of two pregnant stages was performed by the DESeq2 R package (Love et al., 2014). Transcripts with absolute log2 Fold Change values greater than 1 and q-value<0.05 were marked as

differentially expression genes (DEGs).

2.5. Functional annotation and enrichment analysis of DEGs

The genome-wide functional annotation of DEGs was designated by eggNOG-mapper pipeline (https://eggnog-mapper.embl.de/). Gene Ontology (GO) and Kyoto Encyclopedia of Genes and Genomes database (KEGG) enrichment analysis of DEGs were implemented by the ClusterProfiler R package (Yu et al., 2012). The GO terms were classified into official classifications, including molecular function (MF), cellular component (CC), and biological process (BP). The false discovery rate (FDR) was calculated for each *p*-value, and FDR < 0.05 were the criteria for recognizing the significance enriched categories.

2.6. Identification and sequence analysis of black rockfish sema genes

Based on an E-value of $1e^{-10}$, the amino acid sequence of *sema* genes in human (*Homo sapiens*), zebrafish (*Danio rerio*) and guppy (*Poecilia reticulata*) were obtained from the NCBI database and used as queries for BLAST program to identify *sema* genes in black rockfish. Open reading frames (ORF) of candidate black rockfish *sema* genes were predicted by ORFfinder program (https://www.ncbi.nlm.nih.gov/orffinder/), and the ORFs were translated into amino acid sequences. Physicochemical properties such as amino acid length, theoretical isoelectric points (pI) and molecular weight (MW) were predicted by online ExPASy - ProtParam tool (https://web.expasy.org/protparam).

The exon–intron structures of *sema* genes were extracted from the general feature format (GFF) of black rockfish reference genome. The conserved domains and motifs were predicted from Conserved Domains Database (CDD) and Resources (https://www.ncbi.nlm.nih.gov/Structure/cdd) and MEME suite (https://meme-suite.org/meme/doc/meme.html), respectively.

2.7. Phylogenetic and syntenic analysis of black rockfish SEMA

Multiple alignments of amino acid sequences were performed based on semaphorins amino acid sequences of several representative species using ClustalW online program (https://www.genome.jp/tools-bin/clustalw). The phylogenetic tree was reconstructed by multiple alignments of deduced amino acid sequences using MEGA X software based on the Neighbor-Joining (NJ) method and Jones-Taylor-Thornton (JTT) model with bootstrap value setting as 1,000.

Information of chromosome distribution and homology regions, based on reference genome of black rockfish, were accessed by TBtools software (Chen et al., 2020). Collinearity between genomes was analyzed by comparing the chromosomal distribution of black rockfish, guppy and zebrafish. Chromosomal position information of *sema* genes was obtained from the annotation files of the guppy reference genomes (PRJNA238429) and zebrafish reference genomes (PRJNA11776). TBtools Super Circos software was used to visualize the chromosome location and collinearity relationship.

2.8. Experimental validation by qPCR

9 DEGs were selected from transcriptomic data for qPCR verification. Gene-specific primers were listed (**Supplementary Table. S5**). First-strand cDNA was synthesized from 1.0 μg of total pure RNA using the SPARK script 1st Strand cDNA Synthesis Kit (With gDNA Eraser, SparkJade, China). qPCR reaction was performed in a 96-well optical plate and pre-denaturation at 95 °C for 3 min, 40 cycles of denaturation at 95 °C for 10 s and annealing at 60 °C for 30 s on a StepOne PlusTM real-time PCR system (Applied Biosystems, Waltham, Massachusetts, USA) using 2 × SYBR Green qPCR Mix (High ROX, SparkJade, China). 18 s rRNA was used as a reference gene to normalize the expression levels (Liman et al., 2013). The relative expression levels for each gene in F and S stages were quantified according to $2^{-\Delta\Delta CT}$ method with reference to the M and F stage， respectively.

3. Results

3.1. RNA-seq data analysis

According to the previous identification results, 9 libraries were constructed and sequenced from 27 samples in 3 pregnant stages (M, F, S). Utilizing the Illumina HiSeq X Ten platform, a total of 393,596,444 raw reads were generated. After preprocessing and removing low-quality sequences, 389,403,178 clean reads were obtained. Each of these samples comprised at least 42 million reads, of which more than 94.7 and 90% were totally and uniquely mapped to the genome, respectively (**Supplementary Table. S1**). The read counts and FPKM values for all genes were calculated. In total, 24,094 expressed genes were detected from the transcriptome dataset.

3.2. Different expression analysis and functional annotation

To identify differently expressed genes involved in the development of capillaries around embryos, we subjected the expression values to pairwise comparisons, F vs M, S vs M, S vs F. Genes with *q*-value < 0.05 and |log2 Fold Change|greater than1 were considered as DEGs. The results demonstrate that 1,579 DEGs (714 up-regulated and 865 down-regulated) were found in F vs M group, 2,771 DEGs (2,052 up-regulated and 718 down-regulated) were found in S vs M group, and 7,237 DEGs (3,965 up-regulated and 3,272 down-regulated) were found in S vs F group (Fig. 1**A-C**). Venn diagram and Upset diagram showed that a total of 142 genes were found to be differentially expressed in all comparisons (Fig. 1**D**). In addition, 181, 568 and 4,054 DEGs were expressed exclusively in F vs M group, S vs M group and S vs F group, respectively. According to the heatmap, M stage and F stage showed roughly similar expression pattern, which is opposite to S stage (Fig. 1**E**).

GO enrichment analysis was performed to define and describe gene and protein functions. In this study, 30 significant enriched GO terms (*p* adjust < 0.01) were screened in S vs F group and F vs M group, respectively (**Supplementary Table. S2**). Compared with M stage, significantly up-regulated enriched GO terms in F stage were mainly associated with *Immune*, *Molecular transport* and *Metabolism* (Fig. 2**A**). Down-regulated DEGs in F vs M group were significantly enriched in GO terms related to *Meiotic*, *DNA replication*, *Chromosome*, *Molecular transport*, and *Cytoskeleton* (Fig. 2**B**). Compared with F stage, up-regulated DEGs in S stage were mainly overrepresented with GO terms related to *RNA process*, *DNA replication* and *Chromosome* (Fig. 2**C**). Additionally, terms associated specifically with *Immune*, *Cell junction* and *Membrane* were also found in down-regulated DEGs in S vs F group (Fig. 2**D**).

A more profound understanding of functions and processes of the biological system were performed by KEGG pathway enrichment analysis. In the present study, 18 and 20 significant enriched pathways (*p* adjust < 0.01) were screened in S vs F group and F vs M group, respectively (**Supplementary Table. S3**). Compared with M stage, significantly up-regulated KEGG pathways in F stage were mainly classified into 2 categories: *Metabolism* and *Immune* (Fig. 3**A**), while the down-regulated KEGG pathways were enriched for *DNA replication and repair* (Fig. 3**B**). KEGG Pathways up-regulated in S vs F group were significantly enriched for *Cell cycle*, *Metabolism*, *RNA process* and *DNA repair and replication* (Fig. 3**C**). Whereas the expression of DEGs involved in *Immune*, *Cell junction* and *Signal transduction* were down-regulated in S stage in comparison with F stage (Fig. 3**D**).

3.3. KEGG pathways are altered in ovary matrix at sarcomere period

Considering that S vs F group showed most abundant DEGs, indicating various and complex physiological changes appear to occurred in ovary matrix during pregnancy. We focused on KEGG pathways in the S vs F group and compared their expression (Fig. 4). Due to the increased

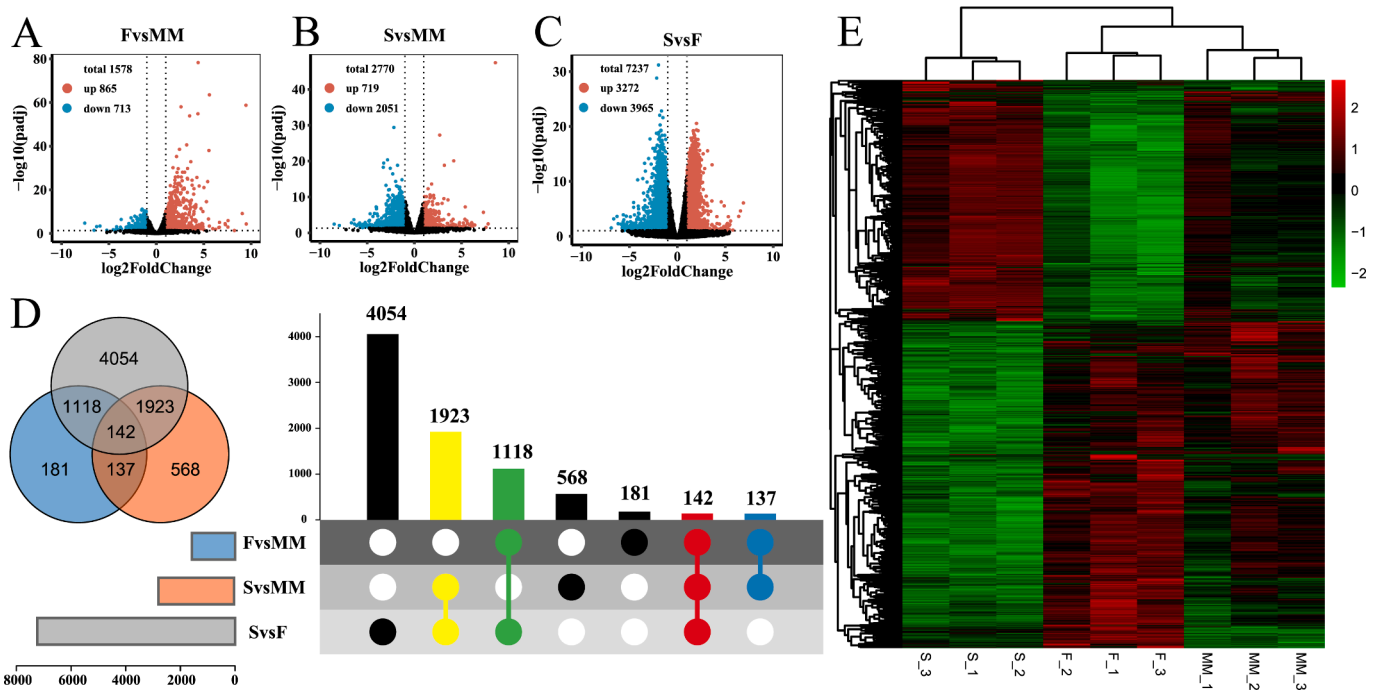

Fig. 1. Analysis of DEGs. A-C: Volcano plots of DEGs in the pairwise comparisons, Red and blue dots indicate significant up-regulation and down-regulation of genes, respectively, while black dots indicate non-significantly DEGs; D: Venn diagram and Upset diagram of the DEGs in 3 comparisons, points connected by a line indicating an intersection in a comparison group; E: Cluster analysis and heatmap. A Heatmap showing expression pattern of DEGs in each sample based on FPKM values (according to the F-test *p*-value from the linear model fit), Green represents down-regulated expression and Red represents up-regulated expression.

cell proliferation, differentiation, and protein synthesis from F stage to S stage, as pregnancy goes by, the category *Cell proliferation* were most significantly overexpressed including "Cell cycle", "DNA replication", "Ribosome biogenesis in eukaryotes", "Oocytes meiosis", "RNA degradation", "RNA polymerase", "RNA transport", "Cellular senescence". Additional pathways related specifically with *DNA damage checkpoints and repairment* were also elevated. Cell-cell interactions pathways involved in *cell junction*, *adherens junction*, *cell adhesion molecules (CAMs)*, *focal adhesion*, and *ECM-receptor interaction* were down-regulated at the S stage, suggesting an probable increase in the ability of cells to migrate and invade. In the category of metabolism, "Cysteine and methionine metabolism" "One carbon pool by folate" "Terpenoid backbone biosynthesis" and "Ubiquitin mediated proteolysis" were up-regulated at S stage compared to F stage, while "Inositol phosphate metabolism" was down-regulated, demonstrating the complex metabolic processes might be occur during pregnancy. When comparing S stage and F stage, the down-regulation pathways involved in immune seemed to prevent the maternal from rejecting the fetus during pregnancy.

3.4. Degs related to capillary angiogenesis on embryo surface

A more specific identification of the genes connected to angiogenesis-related pathways is necessary to learn more about the proliferation of capillaries covering embryos during pregnancy. DNA replication, RNA transcription, and protein synthesis were essential steps in the process of cell proliferation. Our RNA-seq data revealed an increase in vascular development-related DEGs and pathways at the S stage, which suggests that endothelial cells in the ovary matrix proliferated and expanded to produce capillaries. For example, the expression levels of genes encoding Cyclin-dependent kinases (CDKs), mini-chromosome maintenance proteins (MCMs), RNA replicase polyprotein (POLRs), ribosomal protein (MRPLs) were up-regulated at S stage than F stage (**Supplementary** Table. S4). Degradation of extracellular matrix, the diminishing of cell connections and reorganization of actin cytoskeleton facilitate the movement and invasion of capillaries. In our study, DEGs coding proteins involved in *Cell migration and invasion* included matrix metalloproteinase (MMPs) were upregulated after fertilization, while integrin (ITGs), cadherins (CDHs) were shown to be down-regulated at S stage compared to F stage (**Supplementary** Table. S3). The growth of capillaries was regulated by multiple stimulating or inhibiting factors. Among DEGs, common angiogenic factors such as vascular endothelial growth A (VEGFA), erythropoietin (EPO), platelet-derived growth factor (PDGF), C-X-C motif chemokine 8 (CXCL8) presented up-regulation after fertilization (**Supplementary** Table. S3). Interestingly, our transcriptome data revealed significant variations in a number of semaphorin gene family (a class of vascular developmental regulators) members, with 7 of them up-regulated and 9 of them down-regulated during S stage compared to F stage (Table. 1), which deserves further study.

3.5. Identification and analysis of sema genes in black rockfish

Subsequently, a comprehensive analysis of gene identification, gene structure and evolutionary characteristics was conducted to systematically study the Sema family of genes in black rockfish. A total of 32 *sema* genes were identified in black rockfish. The *sema* genes were classified into 5 subfamilies: 12 *sema* genes in subfamily 3 (*sema3aa, sema3ab, sema3b, sema3c, sema3da, sema3db, sema3e, sema3fa, sema3fb, sema3fc, sema3g, sema3h*), 11 *sema* genes in subfamily 4 (*sema4aa, sema4ab, sema4ba, sema4bb, sema4c, sema4d, sema4ea, sema4eb, sema4f, sema4ga, sema4gb*), 2 *sema* genes in subfamily 5 (*sema5ba, sema5bb*), 6 *sema* genes in subfamily 6 (*sema6a, sema6ba, sema6bb, sema6ca, sema6cb, sema6d*) and 1 *sema* gene in subfamily 7 (*sema7a*). The predicted amino acids lengths of *sema* genes ranged from 526 to 1,451, the molecular weights (MWs) were varied from 59.72 kDa to 161.01 kDa and the predicted isoelectric point (PI) varied from 5.64 to 8.83 (Table. 2).

Phylogenetic analysis was constructed using the amino acid sequences of *sema* genes in black rockfish and several mammals, birds, amphibian, teleost and invertebrate (Fig. 5). According to the topology

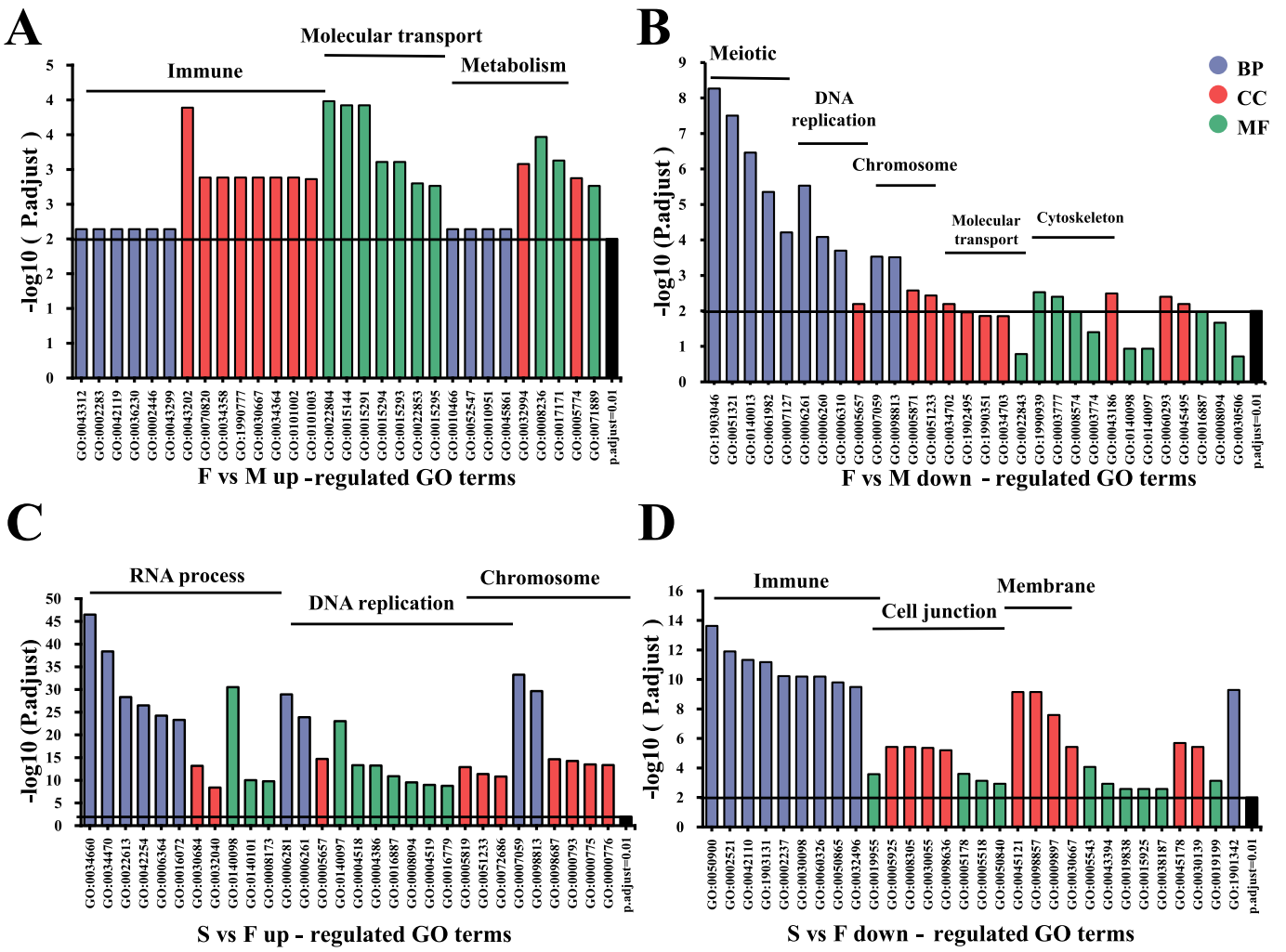

Fig. 2. GO enrichment analysis of DEGs. A: Bar plot of GO enrichment analysis of up-regulated DEGs in F vs M, the top 30 most significantly enriched categories are presented (q-value < 0.05). The blue columns represent the biological process group, the red columns represent the cellular component group, and the green columns represent the molecular function group; B: Bar plot of GO enrichment analysis of down-regulated DEGs in F vs M; C: Bar plot of GO enrichment analysis of up-regulated DEGs in S vs F; D: Bar plot of GO enrichment analysis of down-regulated DEGs in S vs F.

of phylogenetic tree, all *sema* genes were separated into five separate clades and were clustered together with counterparts as expected. It was noteworthy that teleost were home to far more numbers of various *sema* gene subtypes than higher vertebrates. As a result, *sema* genes were mostly preserved throughout the evolution of vertebrates, and their copy number rose in teleost. Chromosomal distribution results showed that *sema* genes in black rockfish were distributed among 15 chromosomes (chrs), including chr1, chr2, chr4, chr5, chr6, chr7, chr11, chr12, chr13, chr16, chr18, chr20, chr21, chr22 and chr23 (**Supplementary** Fig. S2**A**). Comparative genomic analysis showed that tandem arrangements and duplication of *sema* genes were also detected in the genomes of guppy and zebrafish (**Supplementary** Fig. S2**B**).

3.6. Gene structure, conserved motifs and protein structure analysis of sema in black rockfish

To further study the diversity and conservatism, the exon–intron architecture, conserved motifs, and conserved domains of Sema in black rockfish were demonstrated and compared (Fig. 6). Results showed that the majority of the class 3 *sema* genes subfamily members, with the exception of sema3fc, have 16–18 exons. Among class 4 *sema* genes subfamily, the number of exons ranged from 13 to 15, while class 6 *sema* genes subfamily contained 14–18 exons. Besides, 14, 25 and 22 exons existed in *sema7a, sema5ba* and *sema5bb*, respectively (Fig. 6**C**). All semaphorins had a highly conserved Sema domain located at N-terminal and a Plexin-sema-integrin (PSI) domain was next to the C-terminal of Sema domain. Additionally, an Immunoglobulin-like (Ig-like) domain was contained solely in class 3 and 4 Sema and multiple Thrombospondin 1 (TSP1) domains were founded exclusively in class 5 Sema (Fig. 6**B**). In total, ten conserved motifs of Sema in black rockfish were identified (Fig. 6**A**), and the distribution and characteristics of motifs in the same *sema* genes subfamily were analogous. The results indicated that motif 1, 3, 4, 5, 6, 8, 9, and 10 were found in Sema domain, and motif 2 and 7 were defined in PSI domain.

3.7. Expression patterns of sema genes at 3 pregnant stages in black rockfish

The expression profile of *sema* genes was constructed in order to investigate how *sema* genes react to pregnancy signals. (Fig. 7). Based on the expression levels and hierarchical clustering information, these *sema* genes were clustered as high, moderate and low expression. The expression level of the *sema* genes included *sema3da, sema3fc, sema4aa, sema4ba, sema4c, sema4eb, sema6cb* and *sema7a* were maintained at a relatively high level at 3 pregnant stages, indicated they were appeared to be highly relevant to the embryo angiogenesis. On the contrary, the

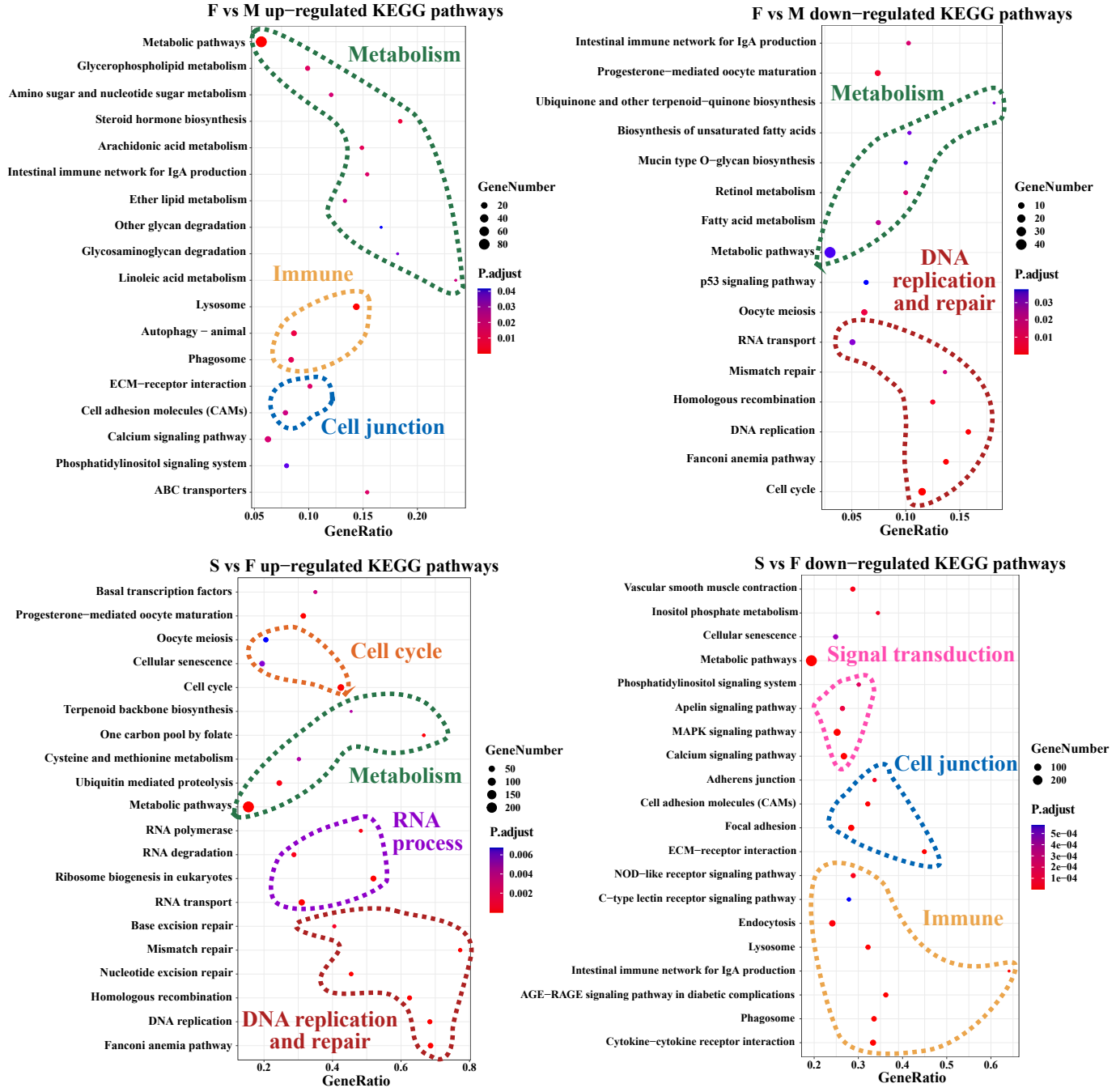

Fig. 3. KEGG enrichment analysis of DEGs. A: Scatterplot of KEGG pathway enrichment analysis of up-regulated DEGs in F vs M. The "GeneRatio" represents the ratio of the differentially expressed gene number to the total gene number in a certain pathway. Top 18 most significantly enriched categories are presented (q-value < 0.05); B: Scatterplot of KEGG pathway enrichment analysis of down-regulated DEGs in F vs M, top 18 most significantly enriched categories are presented; C: Scatterplot of KEGG pathway enrichment analysis of up-regulated DEGs in S vs F, top 20 most significantly enriched categories are presented; D: Scatterplot of KEGG pathway enrichment analysis of down-regulated DEGs in S vs F, top 20 most significantly enriched categories are presented.

abundance of other several *sema* genes, such as *sema3ab*, *sema3fb*, *sema3h*, *sema4f*, *sema4ga*, *sema4gb*, *sema6a*, *sema6ba*, *sema6bb* and *sema6d* were maintained at a low level.

3.8. Validation of transcriptomicresults by qPCR

To validate the RNA-Seq data, 9 DEGs were randomly selected and subjected to qPCR analysis. The results showed that the qPCR expression pattern of the selected genes was significantly correlated with the RNA-Seq results of F vs M (R^2:0.8538) and S vs F (R^2:0.8213) (Fig. 8). In total, the RNA-Seq data were confirmed by the qPCR results, implying the reliability and accuracy of the RNA-Seq analysis.

4. Discussion

Animals evolved their reproductive strategies from oviparity to viviparity to adapt to keep the continuation of species, despite with an increase in parental investment in offspring (Gross, 2005). Ovoviviparity is a reproductive strategy evolved between oviparity and vivipary, with advantages in extending the time a fertilized egg spends developing inside the maternal body, which ensure the health and growth of the offspring (Wake, 2015). In mammals, chorionic and

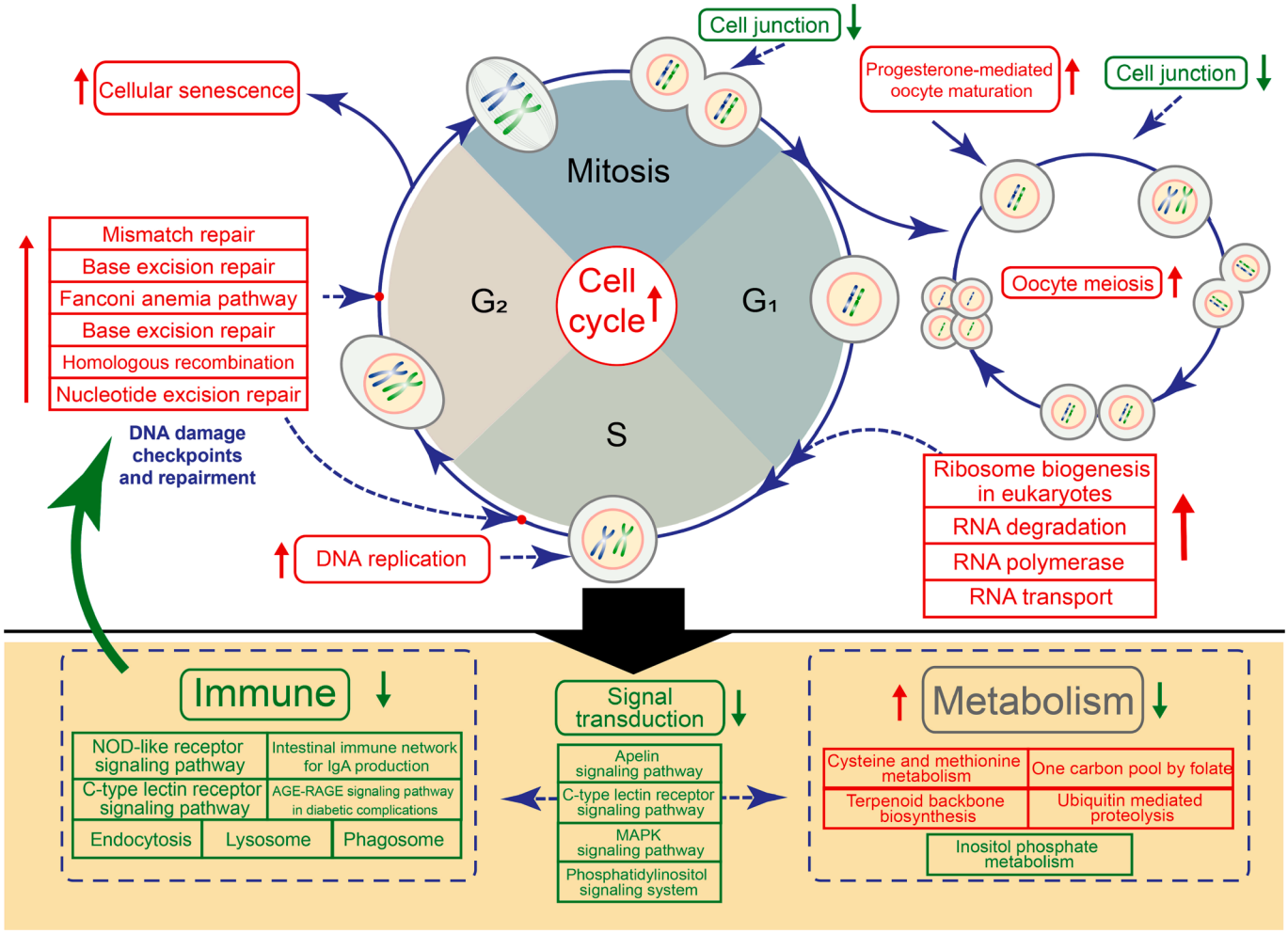

Fig. 4. Overview of significantly enriched KEGG pathways in S vs F. Red and green orthogons represent up-regulated and down-regulated pathways, respectively.

allantoic structures in the placenta were developed to provide nutrition and oxygen for the embryo and fetus development. Similar vascular network in the yolk sac was also observed in lower vertebrate lizard (Stewart and Thompson, 2017), as a result, except birds, placentas have evolved within every vertebrate class (Roberts et al., 2016). In black rockfish, the capillaries increased dramatically with the embryo development and formed a cap shape network, which cover up to half of the embryo, indicating the existence of the substantial deliver system. According to the results, we collected the ovary matrix without oocyte or embryos, at three time points, including mature oocyte, fertilized oocyte and sarcomere period for further transcriptomic analysis, aimed to figure the potential regulation pathways in the formation of the extra-embryonic capillaries.

In our study, abundant DEGs were found after fertilization, suggesting that the ovaries responded more actively and dramatically as pregnancy went by. As compared to pre-fertilization period, significantly higher number of DEGs participated in assorted biological processes including cell proliferation, cell interaction, nutritional metabolism at post-fertilization period based on KEGG analysis. Up-regulation of "Calcium signaling pathway" revealed activation of diverse physiological processes. In black rockfish, oocytes mature and the sperms stored under the ovigerous lamellae epithelium was released to combine the oocytes in April (Kawaguchi et al., 2008). Release of calcium ions from oocytes after sperm fusion is the key to meiosis reactivation (Boni et al., 2007). Transporting through the placenta, calcium regulates massive cellular processes such as genes expression, cell proliferation, differentiation and apoptosis (Baczyk et al., 2011; Berridge et al., 2003). It has been well documented that, to guarantee the proper function of placenta, the interactions between trophoblast cells and the maternal vascular system were enhanced (Adamson et al., 2002; Harris, 2010). Herein, our study found that pathways involved in cellular communication such as "ECM-receptor interaction", "Adherents junction", "Cell adhesion molecules (CAMs)", "Focal adhesion" were up-regulated to higher levels after fertilization. Since the ovary matrix undergoing a series of changes in cell type preprogramme and expressing gene variation (Xu et al., 2022), the "Cell cycle", "DNA replication", "Ribosome biogenesis in eukaryotes", "RNA degradation", "RNA polymerase", "Mismatch repair", "Base excision repair", "Fanconi anemia pathway", "Homologous recombination" and "Nucleotide excision repair" related genes were enriched in our results. On the other hand, to provide enough nutrition for the embryo development, pregnant maternal change the lipid and protein synthesis to supply the essential materials for the embryo (Herrera, 2002). In our data, DGEs and enriched pathways such as lipid and protein synthesis such as "aminoacyl-tRNA biosynthesis", "fatty acid biosynthesis", "steroid hormone biosynthesis" were significantly enhanced with the embryo development. These results indicated that with the fertilization, ovary matrix cells were reprogrammed to fit the requirement of the embryos not only in regulating genes expression, but also in the materials biosynthesis.

During pregnancy, oxygen is necessary for the survival of embryos (Carter, 2015; Harvey, 2007). Due to the large amount and in vivo development, black rockfish embryos are usually exposed to hypoxic environment. Thus, many animals developed morphological and

Table 1
Differential expression multiples of semaphorins involved in angiogenesis in three comparison groups.

Geneid	GeneName	log2FoldChange FvsM	SvsM	SvsF
evm.model.Chr21.288	*sema3aa*	−1.09904	−1.58130	
evm.model.Chr5.849	*sema3ab*			
evm.model.Chr7.685	*sema3b*			
evm.model.Chr21.178	*sema3c*			
evm.model.Chr5.847	*sema3da*	−1.00841	1.07805	2.08645
evm.model.Chr1.1809	*sema3db*			
evm.model.Chr5.851	*sema3e*	1.87627		−1.02851
evm.model.Chr1.1388	*sema3fa*			
evm.model.Chr1.2436	*sema3fb*			
evm.model.Chr7.596	*sema3fc*			−1.16478
evm.model.Chr7.684	*sema3g*		−1.06045	−1.49835
evm.model.Chr7.714_evm.model.Chr7.715	*sema3h*			
evm.model.Chr16.26	*sema4aa*			
evm.model.Chr16.3	*sema4ab*		−1.14860	−1.46307
evm.model.Chr2.915	*sema4ba*			
evm.model.Chr5.777	*sema4bb*			−1.23941
evm.model.Chr6.795	*sema4c*	−1.19448		1.83393
evm.model.Chr1.994	*sema4d*		1.03002	1.94162
evm.model.Chr11.879.1	*sema4ea*			
evm.model.Chr4.770	*sema4eb*			
evm.model.Chr20.570	*sema4f*			
evm.model.Chr12.564	*sema4ga*		−2.15715	−1.63847
evm.model.Chr18.350	*sema4gb*	−1.11872		1.63695
evm.model.Chr13.1156_evm.model.Chr13.1159	*sema5ba*	−1.04135		1.86655
evm.model.Chr23.545	*sema5bb*		1.00257	1.97194
evm.model.Chr6.868	*sema6a*	1.51715		−1.19221
evm.model.Chr4.758	*sema6ba*			−1.14771
evm.model.Chr11.884	*sema6bb*			
evm.model.Chr22.221	*sema6ca*			
evm.model.Chr16.224	*sema6cb*		1.14888	1.29351
evm.model.Chr2.1098	*sema6d*			
evm.model.Chr5.705	*sema7a*	1.81842		−2.15111

Table 2
Characteristics of *sema* genes in black rockfish.

Subfamily classification	Gene Name	CDS length (bp)	Predicted Protein Length (Amino Acid)	Isoelectric point (PI)	Molecular weight (KDa)
Sema3	*sema3aa*	2604	867	8.53	96.61
	sema3ab	2403	800	7.15	91.23
	sema3b	2256	751	8.83	84.90
	sema3c	1944	648	7.24	72.90
	sema3da	2424	807	8.52	81,74
	sema3db	2430	809	6.72	91.53
	sema3e	2382	793	7.52	90.28
	sema3fa	2400	799	7.09	90.21
	sema3fb	2775	924	8.01	104.26
	sema3fc	4356	1451	5.91	161.01
	sema3g	2364	787	7.25	89.14
	sema3h	2289	762	8.51	85.36
Sema4	*sema4aa*	2511	836	6.32	92.39
	sema4ab	2724	907	7.29	99.89
	sema4ba	2514	837	6.35	94.30
	sema4bb	2427	808	7.45	91.00
	sema4c	2607	868	7.48	96.39
	sema4d	2670	889	5.77	98.53
	sema4ea	2442	813	6.24	90.90
	sema4eb	2433	810	5.64	89.67
	sema4f	2559	852	5.81	92.61
	sema4ga	2688	895	7.26	100.04
	sema4gb	2499	832	8.14	93.50
Sema5	*sema5ba*	3375	1124	6.41	124.95
	sema5bb	3279	1092	6.88	121.37
Sema6	*sema6a*	2826	941	8.09	105.31
	sema6ba	2610	869	8.77	97.15
	sema6bb	2433	810	8.77	88.97
	sema6ca	3273	1090	8.14	120.56
	sema6cb	1773	590	8.12	65.48
	sema6d	3336	1111	8.19	122.18
Sema7	*sema7a*	1851	526	6.17	59.72

biochemical response to adapt to hypoxia (Dunwoodie, 2009; Hickey and Simon, 2006). We observed that as pregnancy went on, capillaries around embryos proliferated constantly and rapidly and this phenotype could be explained by our transcriptome data. In our study, an *epas1* gene involved in oxygen deprivation and several genes responsible for vascular development were induced to greater levels after fertilization. Transcriptional response mediated by hypoxia inducible factor (HIF) is a typical pathway to promote hypoxia tolerance, followed by the expression of downstream genes such as *VEGF*, *PDGF*, *EPO*, etc., to promote the proliferation and migration of vascular ECs (Coma et al., 2011; Dai et al., 2007; Darby and Hewitson, 2016; Grimm et al., 2002; Peng et al., 2021; Spirina et al., 2012). Accumulating evidence indicates that HIFs are linked to the health of pregnancy by regulating the differentiation of trophoblast of placenta (Albers et al., 2019; Kenchegowda et al., 2017). To rescue the cells from hypoxia, angiogenesis was induced by several factors including EPO, eNOS, VEGF, Flt-1 regulated by the HIFs (Coulet et al., 2003; Forsythe et al., 1996; Gerber et al., 1997; Semenza and Wang, 1992). Angiogenesis is a complex process, containing movement, invasion and extension of the vascular endothelial tip cells regulated by a balance between pro-angiogenic and anti-angiogenic guiding signals (Adams and Eichmann, 2010; Eichmann and Thomas, 2013; Sakurai et al., 2012; Tam and Watts, 2010). A key feature of angiogenesis is the increasing quantity of ECs to synthesize newborn tubes and an enhancement in ECs invasion. In our study, DEGs involved in cell proliferation and migration were significantly expressed to produce ECs in angiogenesis. In black rockfish, several DEGs associated with angiogenesis, such as stimulating factors of *vegfa*, *epo*, *pdgf*, *cxcl8* and proteases in ECM degradation *mmp13*, *mmp14*, were highly expressed with the embryo development. In conclusion, our morphological and transcriptomic results suggested that during pregnancy, the ovary's capillaries responded to hypoxia cues by extending and expanding.

Interestingly, in our transcriptome data, several members in the semaphoring family expressed significantly different at 3 pregnancy stages. Semaphorins were verified as guidance signals of both nervous and circulating system. During blood vessels growth, semaphorins regulate the direction of angiogenesis by combining specific receptors on endothelial tip cells (Alto and Terman, 2017b; Goshima et al., 2000). Semaphorins are well-known to play essential role in the development of tumors and pathological vascular development (Neufeld et al., 2016), but little is known about their involvement in ovoviviparous teleost reproduction. A total of 32 *sema* genes were identified from the genomic and transcriptomic databases of black rockfish. Notably, the paraphyletic homologous *sema* genes have evolved in great numbers in vertebrates, which may be connected to their more developed neurological and circulatory system. In black rockfish, sema subtype genes were located in different chromosomes. Compared with higher vertebrates, the numbers of *sema* genes were significantly expanded in most selected teleost, which could be the teleost-specific whole genome duplication (Glasauer and Neuhauss, 2014). Within the same subfamily of *sema* genes in black rockfish, the positions of the protein domains and motifs were relatively conserved. The N-terminal Sema domains were crucial for the activation of their receptors, like plexins and neuropilins, which were mostly found in the neurological and circulatory systems and hinted to the formation of blood vessels and axons (Tamagnone et al., 1999; Zachary, 2014). A Plexin-Sema-Integrin (PSI) domain next to the C-terminal of Sema domain, which is homologous to the chain of integrins and a potential regulator of integrin activation (Zhu et al., 2017). Additionally, an immunoglobulin-like domain is only presented in class 3 and class 4 *sema* genes, while class 5 *sema* genes contain several thrombospondin (TSP) domains. By directly binding to various receptors

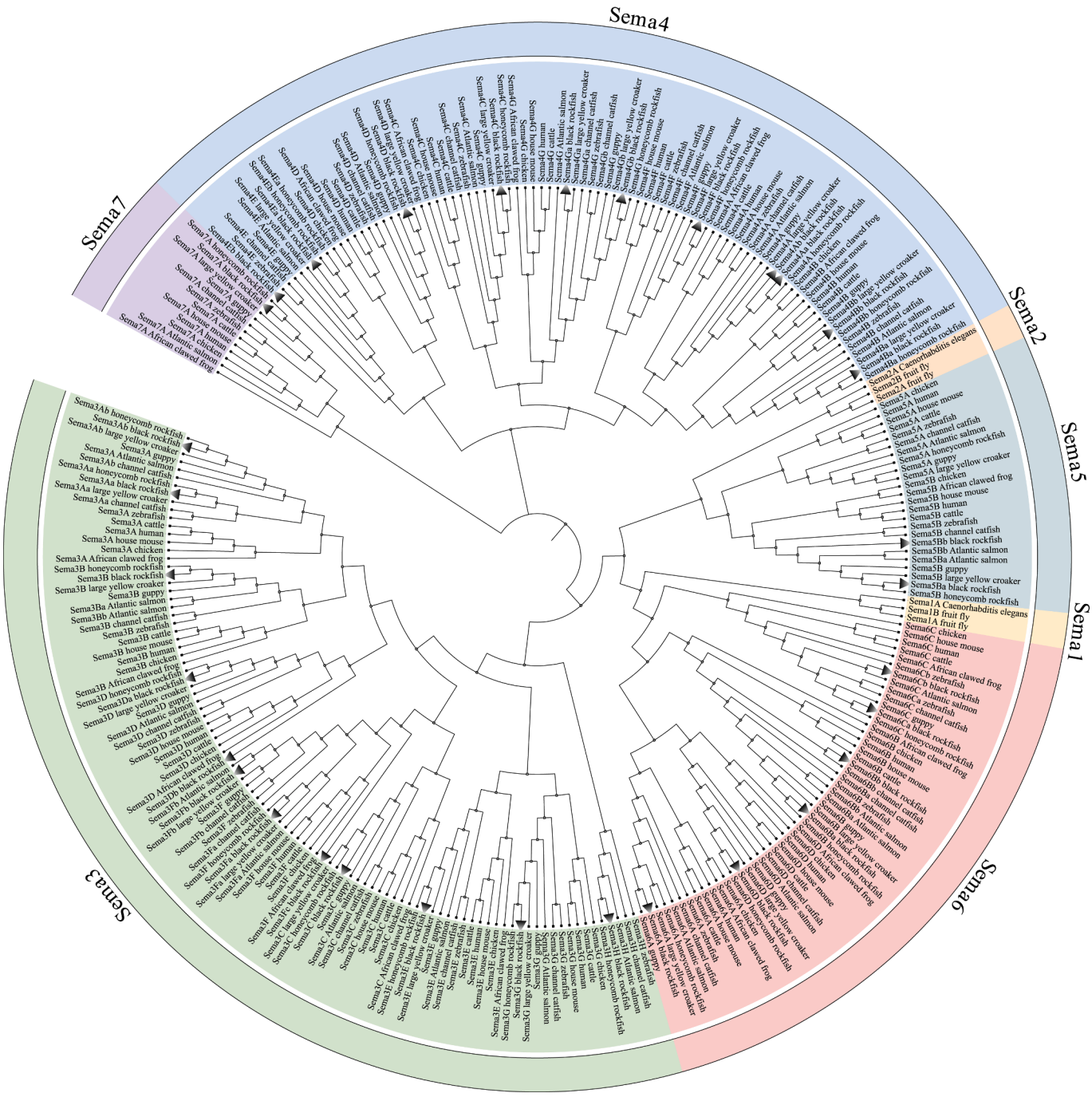

Fig. 5. Phylogenetic relationships of *sema* genes in black rockfish and selected species, including human, mouse (*Mus musculus*), chicken (*Gallus gallus*), cattle (*Bos taurus*), African clawed frog (*Xenopus laevis*), channel catfish (*Ictalurus punctatus*), guppy, large yellow croaker (*Larimichthys crocea*), Atlantic salmon (*Salmo salar*), zebrafish, honeycomb rockfish (*Sebastes umbrosus*) and invertebrate species including Caenorhabditis elegans and fruit fly (*Drosophila melanogaster*). The phylogenetic tree constructed using MEGA X software based on the Neighbor-Joining method and Jones-Taylor-Thornton (JTT) model with 1000 replicates. Semaphorins in black rockfish are indicated by black arrows.

and co-receptors, these domains play a crucial role in the physiological functions of semaphorins. In the glomerular endothelial cells of mouse, Sema3C stimulates integrin-phosphorylated endothelial cell proliferation, migration (Banu et al., 2006). While Sema4D can induce angiogenesis by activating MET receptor in HUVECs (Conrotto et al., 2005).

Semaphorins are important for vascular development by stimulating or inhibiting angiogenesis. The progression of new blood vessel sprouting is determined by a balance between pro- and anti-angiogenic signals. In this study, we performed expression pattern analysis to investigate the potential involvement of *sema* genes during the formation of capillaries around embryos. The majority of Class 3 semaphorins, the only secretory form in vertebrates, might be transferred outside of the cells to exert both healthy and pathological angiogenesis effect (Serini et al., 2009). For example, Sema3A (also known as collapsin-1) inhibited angiogenesis by blocking the proliferation of capillary endothelial cells in vitro in rats (Miao et al., 1999). It also inhibits the undesirable growth of retinal neovascularization and helps to form a well-formed vascular system (Yu et al., 2013). Similarly, Sema3B induced the disintegration of tumor ECs adhesion and actin cytoskeleton, preventing ECs from forming capillaries (Varshavsky et al., 2008).

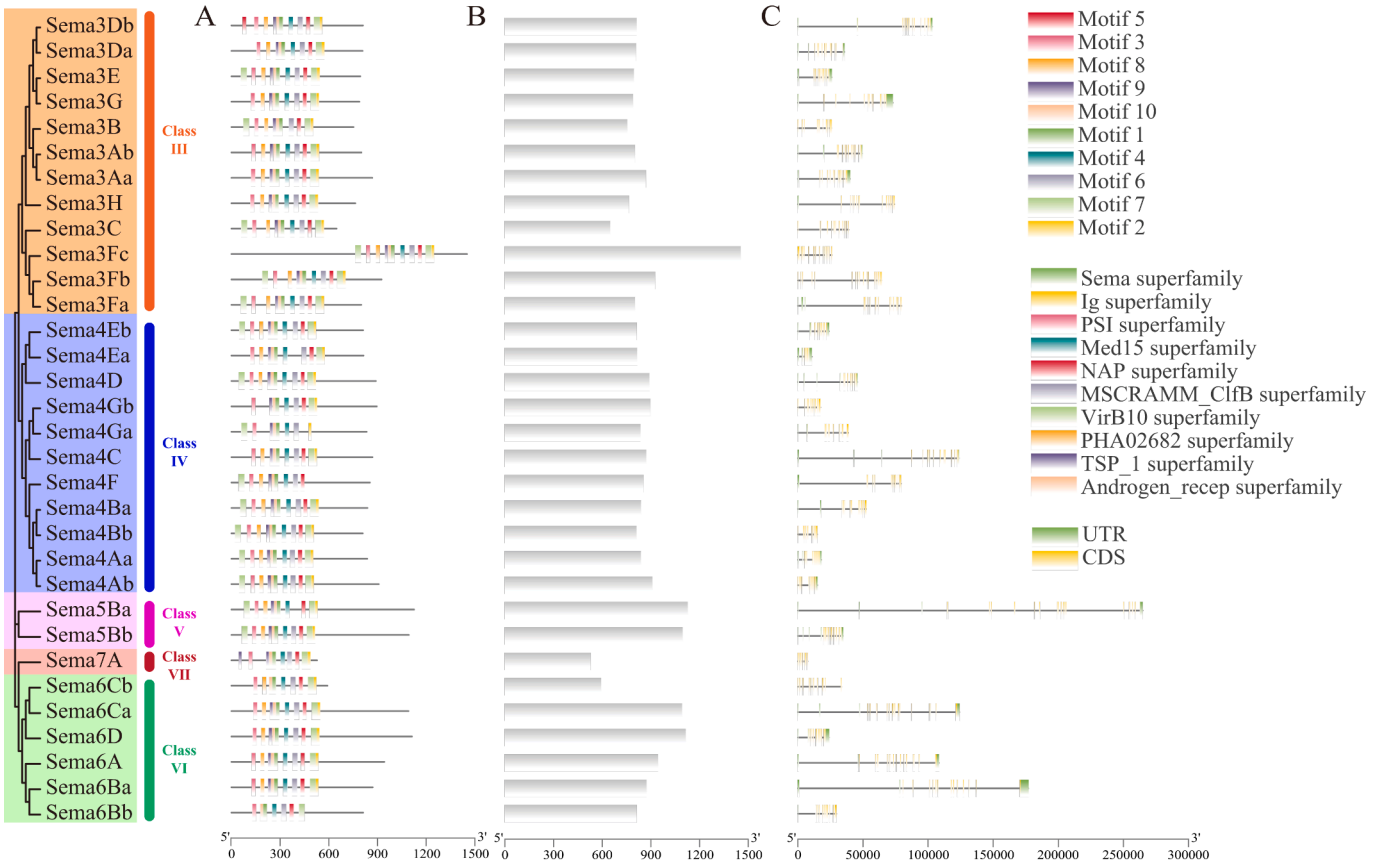

Fig. 6. Schematic representation of conserved motifs. (A), conserved domain (B) and exon–intron structures (C) of *sema* genes in black rockfish. The phylogenetic relationship was shown on the left.

Sema3C inhibits the formation of vascular clusters in retinopathy of prematurity through its receptor Neuropilin-1 and Plexin-D1 (Yang et al., 2015). Sema3F could inhibit tumor cell proliferation, cell adhesion, migration and angiogenesis by blocking VEGF-VEGFR2 signaling pathway (Bielenberg et al., 2004; Kessler et al., 2004). Moreover, Sema3E and Sema3D could suppress the expansion of blood vessels (Aghajanian et al., 2014). However, Sema4D promotes endothelial cell migration, tube formation, vascular permeability, internalization of cadherin and angiogenesis by activating either Plexin-B1 or Plexin-B2 (Conrotto et al., 2005; Wu et al., 2020). Sema4C induced angiogenesis in breast cancer cells by activating the NF-κB pathway (Yang et al., 2019). Interestingly, depending on the surrounding environment, Sema4A present opposite effects in angiogenesis (Meda et al., 2012; Toyofuku et al., 2007). Sema6D and its receptor Plexin-A1 were highly expressed in gastric cancer vascular epithelial cells to activate angiogenesis (Lu et al., 2016). Sema7A is a guiding signal that promotes tumor angiogenesis and induces relevant angiogenic chemokines via α1β1 integrins (Garcia-Areas et al., 2014). In our results, members in the Class 3 semaphorins, including *sema3aa*, *sema3ab*, *sema3b*, *sema3e*, *sema3c*, *sema3db*, *sema3fa*, *sema3fb* showed low expression levels at sarcomere period. While *sema4aa*, *sema4c*, *sema4d* and *sema7a* increased significantly. The semaphoeins identified in our study might be key signaling molecules of pregnant development in black rockfish and merit further study.

5. Conclusion

In conclusion, we were able to confirm that following fertilization, capillaries developed surrounding embryos in the ovary of black rockfish. Comparative transcriptome analysis of three different stages of pregnancy was done to uncover the underlying mechanism. Comprehensive characterization of the expression profiles during pregnancy identified DEGs and key pathways were primarily enriched in cell proliferation and migration, that were crucial for angiogenesis. Among the DEGs, members in semaphorin family were focused since the relevant to angiogenesis. Members of the black rockfish semaphorin family have been identified. Due to genome-wide duplication and tandem duplication events, the semaphorin family has grown because of their great evolutionary conservation. Their various expression patterns might support various angiogenesis-related functions in pregnant black rockfish. Overall, our research provided novel evidence that *sema* genes play a role in the reproductive physiology in ovoviviparity teleost.

Funding information

This study was supported by the National Natural Science Foundation of China (4197608).

Availability of data and material

The results of RNA-seq have been deposited in the Short Read Archive (SRA, https://www.ncbi.nlm.nih.gov/Traces/sra) of the National Center for Biotechnology Information (NCBI) with accession number PRJNA820964.

Declaration of Competing Interest

The authors declare that they have no known competing financial interests or personal relationships that could have appeared to influence the work reported in this paper.

Data availability

No data was used for the research described in the article.

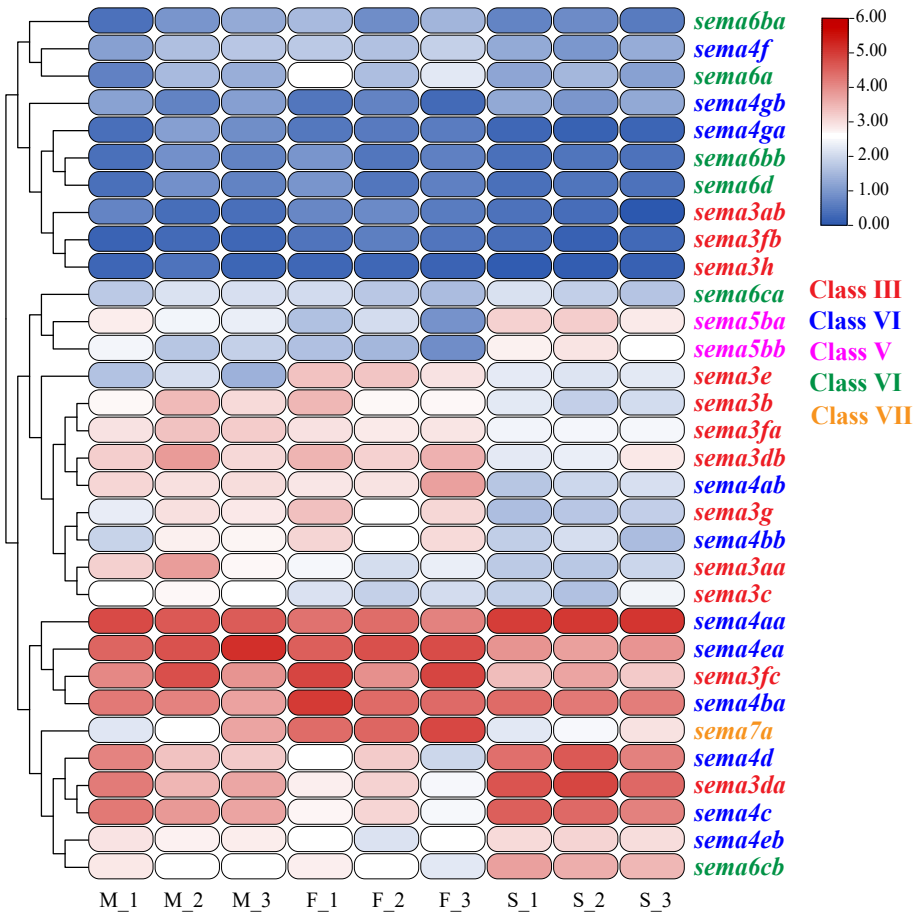

Fig. 7. Temporal expression patterns of *sema* genes in black rockfish at 3 pregnant stages. Data for the relative expression levels of genes are obtained by RNA-seq after taking $\log_2$ (FPKM + 1). The color scale represents expression levels, and red indicate higher expression while blue indicate lower expression.

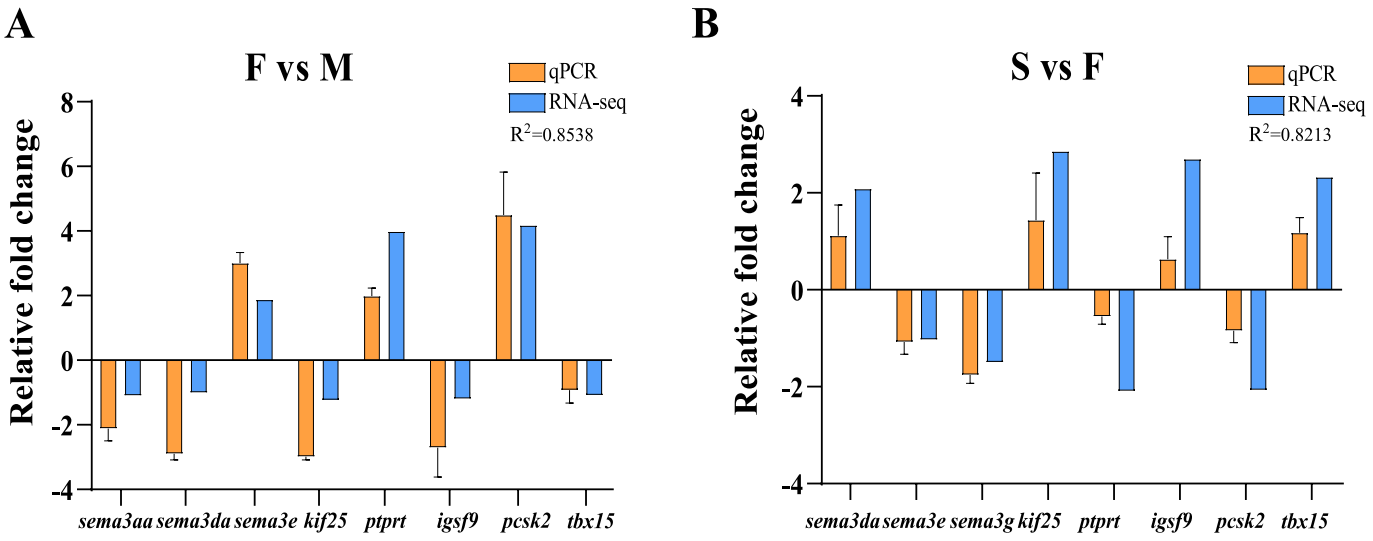

Fig. 8. qPCR validation of 9 DEGs. Relative foldchanges are expressed as the ratio of gene expression after normalizing to reference genes (*18S*). Error bars for qPCR show the standard deviation of three replicates. A: F vs M; B: S vs F. Abbreviation: kinesin family member 25 (*kif25*); protein tyrosine phosphatase receptor type t (*ptprt*); immunoglobulin superfamily member 9 (*igsf9*); proprotein convertase subtilisin kexin type 2 (*pcsk2*); T-Box transcription factor 15 (*tbx15*).

Appendix A. Supplementary data

Supplementary data to this article can be found online at https://doi.org/10.1016/j.ygcen.2023.114275.

References

Adams, R.H., Eichmann, A., 2010. Axon guidance molecules in vascular patterning. Cold Spring Harb. Perspect. Biol. 2, a001875–a. https://doi.org/10.1101/cshperspect.a001875.

Adamson, S.L., Lu, Y., Whiteley, K.J., Holmyard, D., Hemberger, M., Pfarrer, C., Cross, J. C., 2002. Interactions between trophoblast cells and the maternal and fetal circulation in the mouse placenta. Dev. Biol. 250, 358–373. https://doi.org/10.1006/dbio.2002.0773.

Aghajanian, H., Choi, C., Ho, V.C., Gupta, M., Singh, M.K., Epstein, J.A., 2014. Semaphorin 3d and Semaphorin 3e direct endothelial motility through distinct molecular signaling pathways. J. Biol. Chem. 289, 17971–17979. https://doi.org/10.1074/jbc.M113.544833.

Albers, R.E., Kaufman, M.R., Natale, B.V., Keoni, C., Kulkarni-Datar, K., Min, S., Williams, C.R., Natale, D.R.C., Brown, T.L., 2019. Trophoblast-specific expression of Hif-1α results in preeclampsia-like symptoms and fetal growth restriction. Sci. Rep. 9, 2742. https://doi.org/10.1038/s41598-019-39426-5.

Alto, L.T., Terman, J.R., 2017a. Semaphorins and their signaling mechanisms. In: Terman, J.R. (Ed.), Semaphorin Signaling, Methods in Molecular Biology. Springer, New York, New York, NY, pp. 1–25. https://doi.org/10.1007/978-1-4939-6448-2_1.

Baczyk, D., Kingdom, J.C.P., Uhlén, P., 2011. Calcium signaling in placenta. Cell Calcium 49, 350–356. https://doi.org/10.1016/j.ceca.2010.12.003.

Banu, N., Teichman, J., Dunlap-Brown, M., Villegas, G., Tufro, A., Banu, N., Teichman, J., Dunlap-Brown, M., Villegas, G., Tufro, A., 2006. Semaphorin 3C regulates endothelial cell function by increasing integrin activity. FASEB J. 20, 2150–2152. https://doi.org/10.1096/fj.05-5698fje.

Berridge, M.J., Bootman, M.D., Roderick, H.L., 2003. Calcium signalling: dynamics, homeostasis and remodelling. Nat. Rev. Mol. Cell Biol. 4, 517–529. https://doi.org/10.1038/nrm1155.

Bielenberg, D.R., Hida, Y., Shimizu, A., Kaipainen, A., Kreuter, M., Kim, C.C., Klagsbrun, M., 2004. Semaphorin 3F, a chemorepulsant for endothelial cells, induces a poorly vascularized, encapsulated, nonmetastatic tumor phenotype. J. Clin. Invest. 114, 1260–1271. https://doi.org/10.1172/JCI21378.

Boehlert, G.W., Yoklavich, M.M., 1984. Reproduction and embryonic development of the sand tiger shark, *Odontaspis taurus* (Rafinesque). Biol. Bull. 167, 354–370. https://doi.org/10.2307/1541282.

Boni, R., Gualtieri, R., Talevi, R., Tosti, E., 2007. Calcium and other ion dynamics during gamete maturation and fertilization. Theriogenology 68, S156–S164. https://doi.org/10.1016/j.theriogenology.2007.05.048.

Carmeliet, P., 2005. Angiogenesis in life, disease and medicine. Nature 438, 932–936. https://doi.org/10.1038/nature04478.

Carter, A.M., 2015. Placental gas exchange and the oxygen supply to the fetus, in: Terjung, R. (Ed.), Comprehensive Physiology. Wiley, pp. 1381–1403. 10.1002/cphy.c140073.

Chen, C., Chen, H., Zhang, Y., Thomas, H.R., Frank, M.H., He, Y., Xia, R., 2020. TBtools: An Integrative Toolkit Developed for Interactive Analyses of Big Biological Data. Mol. Plant 13, 1194–1202. https://doi.org/10.1016/j.molp.2020.06.009.

Chen, S., Zhou, Y., Chen, Y., Gu, J., 2018. fastp: an ultra-fast all-in-one FASTQ preprocessor. Bioinformatics 34, i884–i890. https://doi.org/10.1093/bioinformatics/bty560.

Coma, S., Shimizu, A., Klagsbrun, M., 2011. Hypoxia induces tumor and endothelial cell migration in a semaphorin 3F- and VEGF-dependent manner via transcriptional repression of their common receptor neuropilin 2. Cell Adhes. Migr. 5, 266–275. https://doi.org/10.4161/cam.5.3.16294.

Conrotto, P., Valdembri, D., Corso, S., Serini, G., Tamagnone, L., Comoglio, P.M., Bussolino, F., Giordano, S., 2005. Sema4D induces angiogenesis through met recruitment by plexin B1. Blood 105, 4321–4329. https://doi.org/10.1182/blood-2004-07-2885.

Coulet, F., Nadaud, S., Agrapart, M., Soubrier, F., 2003. Identification of Hypoxia-response element in the human endothelial nitric-oxide synthase gene promoter. J. Biol. Chem. 278, 46230–46240. https://doi.org/10.1074/jbc.M305420200.

Dai, Y., Xu, M., Wang, Y., Pasha, Z., Li, T., Ashraf, M., 2007. HIF-1α induced-VEGF overexpression in bone marrow stem cells protects cardiomyocytes against ischemia. J. Mol. Cell. Cardiol. 42, 1036–1044. https://doi.org/10.1016/j.yjmcc.2007.04.001.

Darby, I.A., Hewitson, T.D., 2016. Hypoxia in tissue repair and fibrosis. Cell Tissue Res. 365, 553–562. https://doi.org/10.1007/s00441-016-2461-3.

Dunwoodie, S.L., 2009. The Role of hypoxia in development of the mammalian embryo. Dev. Cell 17, 755–773. https://doi.org/10.1016/j.devcel.2009.11.008.

Eichmann, A., Thomas, J.-L., 2013. Molecular parallels between neural and vascular development. Cold Spring Harb. Perspect. Med. 3, a006551–a. https://doi.org/10.1101/cshperspect.a006551.

Folkman, J., 1995. Angiogenesis in cancer, vascular, rheumatoid and other disease. Nat. Med. 1, 27–30. https://doi.org/10.1038/nm0195-27.

Forsythe, J.A., Jiang, B.H., Iyer, N.V., Agani, F., Leung, S.W., Koos, R.D., Semenza, G.L., 1996. Activation of vascular endothelial growth factor gene transcription by hypoxia-inducible factor 1. Mol. Cell. Biol. 16, 4604–4613. https://doi.org/10.1128/MCB.16.9.4604.

Garcia-Areas, R., Libreros, S., Amat, S., Keating, P., Carrio, R., Robinson, P., Blieden, C., Iragavarapu-Charyulu, V., 2014. Semaphorin7A promotes tumor growth and exerts a pro-angiogenic effect in macrophages of mammary tumor-bearing mice. Front. Physiol. 5 https://doi.org/10.3389/fphys.2014.00017.

Gerber, H.-P., Condorelli, F., Park, J., Ferrara, N., 1997. Differential transcriptional regulation of the two vascular endothelial growth factor receptor genes. J. Biol. Chem. 272, 23659–23667. https://doi.org/10.1074/jbc.272.38.23659.

Gilmore, R.G., Dodrill', J.W., Linley', P.A., n.d.,, 1983. Reproduction and embryonic development of the sand tiger shark, *Odontaspis taurus* (Rafinesque). Fis. Bull. 81, 201–225.

Glasauer, S.M.K., Neuhauss, S.C.F., 2014. Whole-genome duplication in teleost fishes and its evolutionary consequences. Mol. Genet. Genomics 289, 1045–1060. https://doi.org/10.1007/s00438-014-0889-2.

Goshima, Y., Sasaki, Y., Nakayama, T., Ito, T., Kimura, T., 2000. Functions of semaphorins in axon guidance and neuronal regeneration. Jpn. J. Pharmacol. 82, 273–279. https://doi.org/10.1254/jjp.82.273.

Graham, S.P., Earley, R.L., Guyer, C., Mendonça, M.T., 2011. Innate immune performance and steroid hormone profiles of pregnant versus nonpregnant cottonmouth snakes (*Agkistrodon piscivorus*). Gen. Comp. Endocrinol. 174, 348–353. https://doi.org/10.1016/j.ygcen.2011.09.015.

Grimm, C., Wenzel, A., Groszer, M., Mayser, H., Seeliger, M., Samardzija, M., Bauer, C., Gassmann, M., Remé, C.E., 2002. HIF-1-induced erythropoietin in the hypoxic retina protects against light-induced retinal degeneration. Nat. Med. 8, 718–724. https://doi.org/10.1038/nm723.

Gross, M.R., 2005. The Evolution of Parental Care. Q. Rev. Biol. 80, 37–45. https://doi.org/10.1086/431023.

Gude, N.M., Roberts, C.T., Kalionis, B., King, R.G., 2004. Growth and function of the normal human placenta. Thromb. Res. 114, 397–407. https://doi.org/10.1016/j.thromres.2004.06.038.

Hanahan, D., Folkman, J., 1996. Patterns and emerging mechanisms of the angiogenic switch during tumorigenesis. Cell 86, 353–364. https://doi.org/10.1016/S0092-8674(00)80108-7.

Harris, L.K., 2010. Review: Trophoblast-vascular cell interactions in early pregnancy: How to remodel a vessel. Placenta 31, S93–S98. https://doi.org/10.1016/j.placenta.2009.12.012.

Harvey, A.J., 2007. The role of oxygen in ruminant preimplantation embryo development and metabolism. Anim. Reprod. Sci. 98, 113–128. https://doi.org/10.1016/j.anireprosci.2006.10.008.

He, Z., Wang, G., Wu, J., Tang, Z., Luo, M., 2021. The molecular mechanism of LRP1 in physiological vascular homeostasis and signal transduction pathways. Biomed. Pharmacother. 139, 111667 https://doi.org/10.1016/j.biopha.2021.111667.

Herrera, E., 2002. Lipid metabolism in pregnancy and its consequences in the fetus and newborn. Endocrine 19, 43–56. https://doi.org/10.1385/ENDO:19:1:43.

Heulin, B., Stewart, J.R., Surget-Groba, Y., Bellaud, P., Jouan, F., Lancien, G., Deunff, J., 2005. Development of the uterine shell glands during the preovulatory and early gestation periods in oviparous and viviparous *Lacerta vivipara*. J. Morphol. 266, 80–93. https://doi.org/10.1002/jmor.10368.

Hickey, M.M., Simon, M.C., 2006. Regulation of angiogenesis by hypoxia and hypoxia–inducible factors, in: Current Topics in Developmental Biology. Elsevier, pp. 217–257. 10.1016/S0070-2153(06)76007-0.

Hota, P.K., Buck, M., 2012. Plexin structures are coming: opportunities for multilevel investigations of semaphorin guidance receptors, their cell signaling mechanisms, and functions. Cell. Mol. Life Sci. 69, 3765–3805. https://doi.org/10.1007/s00018-012-1019-0.

Juntti, S.A., Fernald, R.D., 2016. Timing reproduction in teleost fish: cues and mechanisms. Curr. Opin. Neurobiol. 38, 57–62. https://doi.org/10.1016/j.conb.2016.02.006.

Kawaguchi, M., Nakagawa, M., Noda, T., Yoshizaki, N., Hiroi, J., Nishida, M., Iuchi, I., Yasumasu, S., 2008. Hatching enzyme of the ovoviviparous black rockfish *Sebastes schlegelii*- environmental adaptation of the hatching enzyme and evolutionary aspects of formation of the pseudogene: Hatching enzyme of ovoviviparous black rockfish. FEBS J. 275, 2884–2898. https://doi.org/10.1111/j.1742-4658.2008.06427.x.

Kenchegowda, D., Natale, B., Lemus, M.A., Natale, D.R., Fisher, S.A., 2017. Inactivation of maternal Hif-1α at mid-pregnancy causes placental defects and deficits in oxygen delivery to the fetal organs under hypoxic stress. Dev. Biol. 422, 171–185. https://doi.org/10.1016/j.ydbio.2016.12.013.

Kessler, O., Shraga-Heled, N., Lange, T., Gutmann-Raviv, N., Sabo, E., Baruch, L., Machluf, M., Neufeld, G., 2004. Semaphorin-3F is an inhibitor of tumor angiogenesis. Cancer Res. 64, 1008–1015. https://doi.org/10.1158/0008-5472.CAN-03-3090.

Kim, D., Paggi, J.M., Park, C., Bennett, C., Salzberg, S.L., 2019. Graph-based genome alignment and genotyping with HISAT2 and HISAT-genotype. Nat. Biotechnol. 37, 907–915. https://doi.org/10.1038/s41587-019-0201-4.

Krüger-Genge, B., Franke, J., 2019. Vascular endothelial cell biology: An update. Int. J. Mol. Sci. 20, 4411. https://doi.org/10.3390/ijms20184411.

Liman, M., Wenji, W., Conghui, L., Haiyang, Y., Zhigang, W., Xubo, W., Jie, Q., Quanqi, Z., 2013. Selection of reference genes for reverse transcription quantitative real-time PCR normalization in black rockfish (*Sebastes schlegeli*). Mar. Genomics 11, 67–73. https://doi.org/10.1016/j.margen.2013.08.002.

Lodé, T., 2012. Oviparity or viviparity? That is the question…. Reprod. Biol. 12, 259–264. https://doi.org/10.1016/j.repbio.2012.09.001.

Losordo, D.W., Isner, J.M., 2001. Estrogen and angiogenesis: A review. Arterioscler. Thromb. Vasc. Biol. 21, 6–12. https://doi.org/10.1161/01.atv.21.1.6.

Love, M.I., Huber, W., Anders, S., 2014. Moderated estimation of fold change and dispersion for RNA-seq data with DESeq2. Genome Biol. 15, 550. https://doi.org/10.1186/s13059-014-0550-8.

Lu, Y., Xu, Q., Chen, L., Zuo, Y., Liu, S., Hu, Y., Li, X., Li, Y., Zhao, X., 2016. Expression of semaphorin 6D and its receptor plexin-A1 in gastric cancer and their association with tumor angiogenesis. Oncol. Lett. 12, 3967–3974. https://doi.org/10.3892/ol.2016.5208.

Maltepe, E., Fisher, S.J., 2015. Placenta: The forgotten organ. Annu. Rev. Cell Dev. Biol. 31, 523–552. https://doi.org/10.1146/annurev-cellbio-100814-125620.

Meda, C., Molla, F., De Pizzol, M., Regano, D., Maione, F., Capano, S., Locati, M., Mantovani, A., Latini, R., Bussolino, F., Giraudo, E., 2012. Semaphorin 4A exerts a proangiogenic effect by enhancing vascular endothelial growth factor-A expression in macrophages. J. Immunol. 188, 4081–4092. https://doi.org/10.4049/jimmunol.1101435.

Melincovici, C.S., Bo, A.B., Mihu, C., Istrate, M., Moldovan, I.-M., Roman, A.L., Mihu, C. M., n.d.,, 2018. Vascular endothelial growth factor (VEGF) – key factor in normal and pathological angiogenesis. Rom J. Morphol. Embryol. 59, 455–467.
Miao, H.-Q., Soker, S., Feiner, L., Alonso, J.L., Raper, J.A., Klagsbrun, M., 1999. Neuropilin-1 mediates collapsin-1/semaphorin III inhibition of endothelial cell motility. J. Cell Biol. 146, 233–242. https://doi.org/10.1083/jcb.146.1.233.
Murphy, B.F., Thompson, M.B., 2011. A review of the evolution of viviparity in squamate reptiles: the past, present and future role of molecular biology and genomics. J. Comp. Physiol. B 181, 575–594. https://doi.org/10.1007/s00360-011-0584-0.
Neufeld, G., Mumblat, Y., Smolkin, T., Toledano, S., Nir-Zvi, I., Ziv, K., Kessler, O., 2016. The semaphorins and their receptors as modulators of tumor progression. Drug Resist. Updat. 29, 1–12. https://doi.org/10.1016/j.drup.2016.08.001.
Packard, G.C., Tracy, C.R., Roth, J.J., 1977. The physiological ecology of reptilian eggs and embryos. And the evolution of viviparity within the class reptilia. Biol. Rev. 52, 71–105. https://doi.org/10.1111/j.1469-185X.1977.tb01346.x.
Peng, G., Wang, Y., Ge, P., Bailey, C., Zhang, P., Zhang, D., Meng, Z., Qi, C., Chen, Q., Chen, J., Niu, J., Zheng, P., Liu, Y., Liu, Y., 2021. The HIF1α-PDGFD-PDGFRα axis controls glioblastoma growth at normoxia/mild-hypoxia and confers sensitivity to targeted therapy by echinomycin. J. Exp. Clin. Cancer Res. 40, 278. https://doi.org/10.1186/s13046-021-02082-7.
Pertea, M., Pertea, G.M., Antonescu, C.M., Chang, T.-C., Mendell, J.T., Salzberg, S.L., 2015. StringTie enables improved reconstruction of a transcriptome from RNA-seq reads. Nat. Biotechnol. 33, 290–295. https://doi.org/10.1038/nbt.3122.
Power, M.L., Schulkin, J., 2012. Maternal obesity, metabolic disease, and allostatic load. Physiol. Behav. 106, 22–28. https://doi.org/10.1016/j.physbeh.2011.09.011.
Renfree, M.B., 2010. Review: Marsupials: Placental mammals with a difference. Placenta 31, S21–S26. https://doi.org/10.1016/j.placenta.2009.12.023.
Rheubert, J.L., Siegel, D.S., Trauth, S.E. (Eds.), 2014. Viviparity and placentation in lizards, in: Reproductive Biology and Phylogeny of Lizards and Tuatara. CRC Press, pp. 460–575. 10.1201/b17961-16.
Richeri, A., Chalar, C., Martínez, G., Greif, G., Bianchimano, P., Brauer, M.M., 2011. Estrogen up-regulation of semaphorin 3F correlates with sympathetic denervation of the rat uterus. Auton. Neurosci. Basic Clin. 164, 43–50. https://doi.org/10.1016/j.autneu.2011.06.002.
Roberts, R.M., Green, J.A., Schulz, L.C., 2016. The evolution of the placenta. Reproduction 152, R179–R189. https://doi.org/10.1530/REP-16-0325.
Sakurai, A., Doci, C., Gutkind, J.S., 2012. Semaphorin signaling in angiogenesis, lymphangiogenesis and cancer. Cell Res 22, 23–32. https://doi.org/10.1038/cr.2011.198.
Schindler, J.F., Hamlett, W.C., 1993. Maternal-embryonic relations in viviparous teleosts. J. Exp. Zool. 266, 378–393. https://doi.org/10.1002/jez.1402660506.
Semenza, G.L., Wang, G.L., 1992. A nuclear factor induced by hypoxia via de novo protein synthesis binds to the human erythropoietin gene enhancer at a site required for transcriptional activation. Mol. Cell. Biol. 12, 5447–5454. https://doi.org/10.1128/MCB.12.12.5447.
Serini, G., Maione, F., Bussolino, F., 2009. Semaphorins and tumor angiogenesis. Angiogenesis 12, 187–193. https://doi.org/10.1007/s10456-009-9138-4.
Shine, R., 1989. Ecological causes for the evolution of sexual dimorphism: A Review of the Evidence. Q. Rev. Biol. 64, 419–461. https://doi.org/10.1086/416458.
Spirina, L.V., Yunusova, N.V., Kondakova, I.V., Kolomiets, L.A., Koval, V.D., Chernyshova, A.L., Shpileva, O.V., 2012. Association of growth factors, HIF-1 and NF-κB expression with proteasomes in endometrial cancer. Mol. Biol. Rep. 39, 8655–8662. https://doi.org/10.1007/s11033-012-1720-y.
Stewart, J.R., Thompson, M.B., 2017. Yolk sac development in lizards (Lacertilia: Scincidae): New perspectives on the egg of amniotes. J. Morphol. 278, 574–591. https://doi.org/10.1002/jmor.20656.
Tam, S.J., Watts, R.J., 2010. Connecting vascular and nervous system development: Angiogenesis and the blood-brain barrier. Annu. Rev. Neurosci. 33, 379–408. https://doi.org/10.1146/annurev-neuro-060909-152829.
Tamagnone, L., Artigiani, S., Chen, H., He, Z., Ming, G., Song, H., Chedotal, A., Winberg, M.L., Goodman, C.S., Poo, M., Tessier-Lavigne, M., Comoglio, P.M., 1999. Plexins are a large family of receptors for transmembrane, secreted, and GPI-anchored semaphorins in vertebrates. Cell 99, 71–80. https://doi.org/10.1016/S0092-8674(00)80063-X.
Thompson, M.B., Speake, B.K., 2006. A review of the evolution of viviparity in lizards: structure, function and physiology of the placenta. J. Comp. Physiol. B 176, 179–189. https://doi.org/10.1007/s00360-005-0048-5.
Thompson, M.B., Stewart, J.R., Speake, B.K., 2000. Comparison of nutrient transport across the placenta of lizards differing in placental complexity. Comp. Biochem. Physiol. A. Mol. Integr. Physiol. 127, 469–479. https://doi.org/10.1016/S1095-6433(00)00277-4.
Toyofuku, T., Yabuki, M., Kamei, J., Kamei, M., Makino, N., Kumanogoh, A., Hori, M., 2007. Semaphorin-4A, an activator for T-cell-mediated immunity, suppresses angiogenesis via Plexin-D1. EMBO J. 26, 1373–1384. https://doi.org/10.1038/sj.emboj.7601589.
Tran, T.S., Kolodkin, A.L., Bharadwaj, R., 2007. Semaphorin regulation of cellular morphology. Annu. Rev. Cell Dev. Biol. 23, 263–292. https://doi.org/10.1146/annurev.cellbio.22.010605.093554.
Turner, H.E., Harris, A.L., Melmed, S., Wass, J.A.H., 2003. Angiogenesis in endocrine tumors. Endocr. Rev. 24, 600–632. https://doi.org/10.1210/er.2002-0008.
Varshavsky, A., Kessler, O., Abramovitch, S., Kigel, B., Zaffryar, S., Akiri, G., Neufeld, G., 2008. Semaphorin-3B is an angiogenesis inhibitor that is inactivated by furin-like pro-protein convertases. Cancer Res. 68, 6922–6931. https://doi.org/10.1158/0008-5472.CAN-07-5408.
Wake, M.H., 2015. Fetal adaptations for viviparity in amphibians: Amphibian fetal adaptations. J. Morphol. 276, 941–960. https://doi.org/10.1002/jmor.20271.
Wang, X., Wen, H., Li, Y., Lyu, L., Song, M., Zhang, Y., Li, J., Yao, Y., Li, J., Qi, X., 2021. Characterization of CYP11A1 and its potential role in sex asynchronous gonadal development of viviparous black rockfish *Sebastes schlegelii* (Sebastidae). Gen. Comp. Endocrinol. 302, 113689 https://doi.org/10.1016/j.ygcen.2020.113689.
Wu, J., Li, Y., Chen, A., Hong, C., Zhang, C., Wang, H., Zhou, Y., Li, P., Wang, Y., Mao, L., Xia, Y., He, Q., Jin, H., Yue, Z., Hu, B., 2020. Inhibition of Sema4D/PlexinB1 signaling alleviates vascular dysfunction in diabetic retinopathy. EMBO Mol. Med. 12. 10.15252/emmm.201810154.
Xu, X., Wang, X., Liu, Q., Qi, X., Zhou, L., Liu, H., Li, J., 2022. New insights on folliculogenesis and follicular placentation in marine viviparous fish black rockfish (*Sebastes schlegelii*). Gene 827, 146444. https://doi.org/10.1016/j.gene.2022.146444.
Yang, W., Hu, J., Uemura, A., Tetzlaff, F., Augustin, H.G., Fischer, A., 2015. Semaphorin-3C signals through Neuropilin-1 and PlexinD1 receptors to inhibit pathological angiogenesis. EMBO Mol. Med. 7, 1267–1284. https://doi.org/10.15252/emmm.201404922.
Yang, J., Zeng, Z., Qiao, L., Jiang, X., Ma, J., Wang, J., Ye, S., Ma, Q., Wei, J., Wu, M., Huang, X., Ma, D., Gao, Q., 2019. Semaphorin 4C promotes macrophage recruitment and angiogenesis in breast cancer. Mol. Cancer Res. 17, 2015–2028. https://doi.org/10.1158/1541-7786.MCR-18-0933.
Yin, K.-J., Olsen, K., Hamblin, M., Zhang, J., Schwendeman, S.P., Chen, Y.E., 2012. Vascular endothelial cell-specific microRNA-15a inhibits angiogenesis in hindlimb ischemia. J. Biol. Chem. 287, 27055–27064. https://doi.org/10.1074/jbc.M112.364414.
Yu, W., Bai, Y., Han, N., Wang, F., Zhao, M., Huang, L., Li, X., 2013. Inhibition of pathological retinal neovascularization by semaphorin 3A. Mol. Vis. 19, 1397–1405.
Yu, G., Wang, L.-G., Han, Y., He, Q.-Y., 2012. ClusterProfiler: An R package for comparing biological themes among gene clusters. OMICS J. Integr. Biol. 16, 284–287. https://doi.org/10.1089/omi.2011.0118.
Zachary, I., 2014. Neuropilins: Role in signaling, angiogenesis and disease, in: Marone, G., Granata, F. (Eds.), Chemical Immunology and Allergy. S. Karger AG, pp. 37–70. 10.1159/000354169.
Zhu, G., Zhang, Q., Reddy, E.C., Carrim, N., Chen, Y., Xu, X.R., Xu, M., Wang, Y., Hou, Y., Ma, L., Li, Y., Rui, M., Petruzziello-Pellegrini, T.N., Lavalle, C., Stratton, T.W., Lei, X., Adili, R., Chen, P., Zhu, C., Wilkins, J.A., Hynes, R.O., Freedman, J., Ni, H., 2017. The integrin PSI domain has an endogenous thiol isomerase function and is a novel target for antiplatelet therapy. Blood 129, 1840–1854. https://doi.org/10.1182/blood-2016-07-729400.